Plasmons in disordered, two-component, quasi-two-dimensional electron systems

Mark R. A. Shegelski and D. J. W. Geldart
Department of Physics, Dalhousie University, Halifax, Nova Scotia, Canada B3H 3J5
(Received 13 April 1989)

We investigate the effect of elastic scattering of electrons on properties of plasmons in a disordered, two-component, quasi-two-dimensional electron gas. Numerical results are given for dispersion relations and lifetimes of optical and acoustical plasmons, and for the dynamical structure factor. Acoustical plasmons are destroyed at long wavelength and exist only above a critical wave number q_c, which depends strongly on electron-impurity scattering rates.

I. INTRODUCTION

There has been a recent increase in interest in plasmons in quasi-two-dimensional electron systems. This is partly due to the discovery of high-temperature superconductivity,[1,2] and the associated search for new, nonphonon mechanisms of superconductivity. The increased interest is also related to the experimental search for acoustical plasmons in materials exhibiting quasi-two-dimensional electron dynamics.[3,4] There have been several investigations, within mean-field models, into the possibility that plasmons mediate the attractive electron-electron interaction in high-temperature superconductors.[5–10] Ruvalds has studied the effect of acoustical plasmons within the random-phase approximation (RPA) in quasi-two-dimensional systems and suggested that they may lead to room-temperature superconductivity in La-Ba-Cu-O compounds.[5] Vignale has examined the effect of short-range exchange correlation (beyond RPA) on plasmon dispersion relations and lifetimes, and has concluded that Landau damping allows the existence of acoustical plasmons only below a maximum wave number $q_{\max}$, which can be significantly reduced by strong, short-range correlations.[11] One may also expect elastic electron scattering to be an important source of plasmon damping in view of the nonstoichiometric structure and associated disorder of these materials.

The primary purpose of this paper is to determine how the elastic scattering of electrons from static defects (referred to as impurities) affects the existence, dispersion, and lifetime of acoustical plasmons in a simple, two-component, quasi-two-dimensional electron gas. We find that scattering induces overdamping of plasmons at long wavelength, or $q \lesssim q_c$, where q_c is a critical wave number that increases with the scattering strength (for example, in one of the cases considered below, acoustical plasmons are overdamped for $q \lesssim 0.02 k_h^F$, where k_h^F is the Fermi wave number of the heavy component). Although the dispersion of the surviving plasmons is only slightly affected by scattering, the plasmon lifetimes can be significantly reduced. We also report the effect of impurity scattering on the properties of optical plasmons.

II. MODEL AND METHODS

We consider a quasi-two-dimensional, two-component, degenerate electron gas subject to elastic scattering from static impurities. We model the dispersions of the light and heavy electrons, with effective masses m_l and m_h, respectively, as $\varepsilon_l^k = \hbar^2 k^2/2m_l$ and $\varepsilon_h^k = \hbar^2 k^2/2m_h$, respectively. The Fermi energies are $\varepsilon_j^F = (\hbar k_j^F)^2/2m_j$, where $j=(l,h)$ and the k_j^F are the Fermi wave numbers. We introduce the parameters

$$M = \frac{m_h}{m_l}, \quad K = \frac{k_l^F}{k_h^F}, \quad t = \frac{\tau_h}{\tau_l},$$

where τ_j is the mean free collision time for component j.

The dispersion relations for plasmons in our model are readily seen to be given in the random-phase approximation by

$$\epsilon(q,\omega) = 1 + V_q(\Pi_l^{\rm imp}(q,\omega) + \Pi_h^{\rm imp}(q,\omega)) = 0 , \tag{2.1}$$

where $\epsilon(q,\omega)$ is the dielectric function, $V_q = 2\pi e^2/\epsilon_0 q$, ϵ_0 is the static background dielectric constant, and $\Pi_j^{\rm imp}(q,\omega)$ is the irreducible polarization function of component j in the presence of impurities. We employ the asymptotic form[12] of $\Pi_j^{\rm imp}(q,\omega)$ corresponding to $q \ll k_j^F$, $\hbar\omega \ll \varepsilon_j^F$:

$$\Pi_j^{\rm imp}(q,\omega) = \frac{m_j}{\pi\hbar^2}\left[1 - \frac{\omega}{[(\omega + i/\tau_j)^2 - (q v_j^F)^2]^{1/2} - i/\tau_j}\right] . \tag{2.2}$$

In our investigation of the plasmon dispersion and lifetime, we employ three different methods that are commonly used. Comparison of the results of the three methods is particularly instructive in cases where the lifetime is short.

A. Peaks in the loss function

Well-defined plasmon modes are associated with resonances in the loss function,

$$S(q,\omega) = -\,{\rm Im}\left[\frac{1}{\epsilon(q,\omega)}\right] . \tag{2.3}$$

We determine the plasmon dispersion ω_q and lifetime γ_q directly from the loss function by calculating, for a given value of q, the peak position ω_q and half-width γ_q at half maximum.

B. Weak-damping approximation

The dispersion is approximated by the solution ω_q to

$$\mathrm{Re}\epsilon(q,\omega)=0\ , \tag{2.4}$$

and the lifetime is approximated by its weak-damping form

$$\gamma_q=\mathrm{Im}\epsilon(q,\omega_q)/(\{\partial[\mathrm{Re}\epsilon(q,\omega)]/\partial\omega\}_{\omega=\omega_q})\ . \tag{2.5}$$

The solutions corresponding to plasmons require $\gamma_q>0$.

C. Analytic continuation

The dispersion and lifetime are given by the zeros of the analytic continuation of the (retarded) dielectric function into the lower half of the complex ω plane; that is, by the solutions to the equations

$$\mathrm{Re}\epsilon(q,\omega_q-i\gamma_q)=0\ , \tag{2.6}$$

$$\mathrm{Im}\epsilon(q,\omega_q-i\gamma_q)=0\ . \tag{2.7}$$

These methods will give very similar results and plasmons will be well defined only if $\gamma_q/\omega_q\ll 1$.

We specify the strength of the scattering by a parameter λ, where $\hbar/\tau_j=\varepsilon_j^F/\lambda$ for both $j=l$ and $j=h$, and we rewrite Eq. (2.1) in terms of M, K, λ, and t:

$$1+M+\frac{\tilde{q}}{\tilde{q}_l^{\,\mathrm{TF}}}=\tilde{\omega}\lambda\left[Mt\frac{1}{[(\tilde{\omega}\lambda t+i)^2-(2\tilde{q}\lambda t/MK)^2]^{1/2}-i}+\frac{1}{[(\tilde{\omega}\lambda+i)^2-(2\tilde{q}\lambda)^2]^{1/2}-i}\right]\ , \tag{2.8}$$

where $\tilde{\omega}=\hbar\omega/\varepsilon_l^F$, $\tilde{q}=q/k_l^F$, $\tilde{q}_l^{\,\mathrm{TF}}=q_l^{\mathrm{TF}}/k_l^F$, and $q_j^{\mathrm{TF}}=2e^2m_j/\hbar^2\epsilon_0$ is the Thomas-Fermi wave number for component j.

For each of the three methods described above, we have obtained results by using Eq. (2.8) to solve numerically, via computer, for the dispersion and lifetime. Note that $\tilde{\omega}$ is purely real in each of the first two methods, while $\tilde{\omega}$ is complex in the third method.

We follow Ruvalds[5] and Vignale[11] in choosing $M=3$ and $K=\sqrt{10/3}$ (corresponding to $\varepsilon_l^F/\varepsilon_h^F=10$), which allows for easy comparison between our work and theirs. We consider three different cases for the scattering strength: $\lambda=10$, 100, and 1000. In all three cases, $t=\tau_h/\tau_l=10$. The one parameter left to choose is q_l^{TF} (TF denotes Thomas-Fermi). One can readily show that $\tilde{q}_j^{\,\mathrm{TF}}=\sqrt{2}r_j^s$, where r_j^s is the usual average electron spacing for component j. We follow Vignale in taking $r_h^s=1$. Since $q_h^{\mathrm{TF}}/q_l^{\mathrm{TF}}=M$, this choice fixes q_l^{TF}.

Finally, we choose the range of $\tilde{q}$ we wish to examine. Since Eq. (2.8) involves the asymptotic forms for the $\Pi_j^{\mathrm{imp}}(q,\omega)$ when $q\ll k_j^F$, we choose q so that $q\lesssim k_l^F/3$ and $q\lesssim k_h^F/3$. The latter condition is more restricting and is equivalent to $\tilde{q}\lesssim MK/3t=1/\sqrt{30}$.

III. RESULTS AND DISCUSSION

In Fig. 1 we show the plasmon dispersion as determined by the loss-function method. We show the optical and acoustical branches for the cases $\lambda=10$ and 100, referred to henceforth as $O1$,$O2$ and $A1$,$A2$, respectively (see Fig. 1). The optical and acoustical branches for $\lambda=1000$, $O3$ and $A3$, respectively, are practically indistinguishable from their $\lambda=100$ counterparts, $O2$ and $A2$, and are not shown; the only noteworthy exception is that branch $A3$ extends almost to the origin, whereas branch $A2$ does not (see Fig. 1). Curves $O3$ and $A3$ are essentially those corresponding to $1/\tau_h=1/\tau_l=0$. The dashed curves show the electron-hole–pair excitation boundaries for the light component (steeper line) and the heavy component.

The most striking curve in Fig. 1 is branch $A1$. As we move down this curve (q and ω_q decreasing), we encounter a point, designated by a +, where $\gamma_q/\omega_q=\frac{1}{4}$. This point occurs at $(\tilde{q},\tilde{\omega}_q)=(\tilde{q}_1,\tilde{\omega}_1)\approx(0.14, 0.07)$. Further down the curve, at $(\tilde{q},\tilde{\omega}_q)=(\tilde{q}_2,\tilde{\omega}_2)\approx(0.11, 0.055)$, is a second point, designated by a ●, where $\gamma_q/\omega_q=\frac{1}{2}$. In this paper, we use the term "overdamped" to indicate that $\gamma_q/\omega_q\geq\frac{1}{2}$. Curve $A1$ terminates at $(\tilde{q},\tilde{\omega}_q)=(\tilde{q}_t,\tilde{\omega}_t)\approx(0.053, 0.034)$.

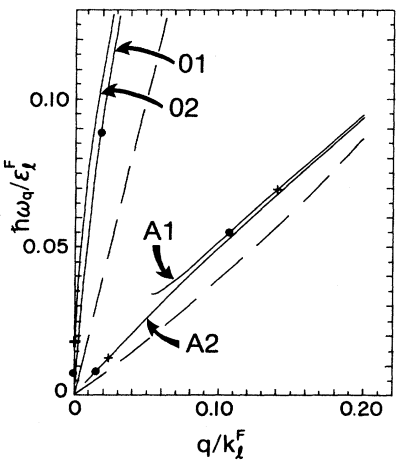

FIG. 1. Plasmon dispersions obtained from peaks in the loss function. The dispersions are labeled $O1$, $O2$, $A1$, and $A2$ for the optical branches in the cases $\lambda=10$ and $\lambda=100$ and for the acoustical branches for $\lambda=10$ and $\lambda=100$, respectively. Points marked + and ● indicate $\gamma_q/\omega_q=\frac{1}{4}$ and $\frac{1}{2}$, respectively. The dashed curves are the electron-hole–regime boundaries for the light component (steep line) and heavy component.

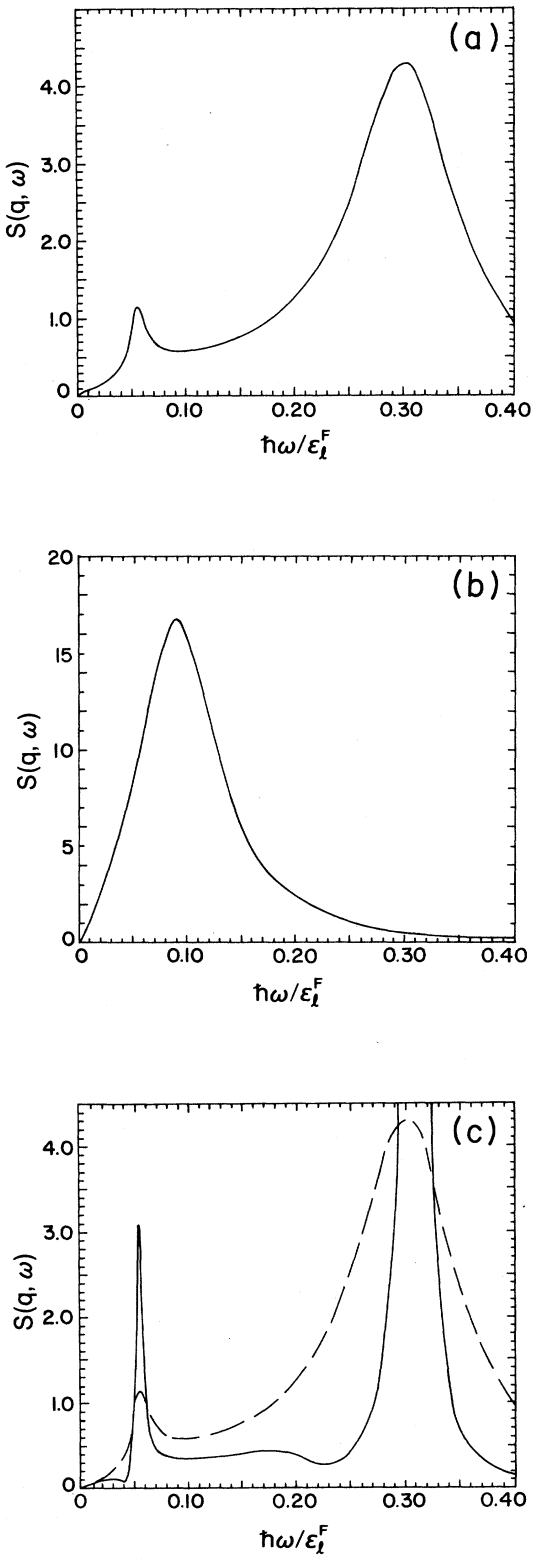

FIG. 2. The loss function $S(q,\omega)$ vs $\hbar\omega/\varepsilon_l^F$ for (a) $\tilde{q}=0.11$, $\lambda=10$; (b) $\tilde{q}=0.0175$, $\lambda=10$; (c) $\tilde{q}=0.11$, $\lambda=10$ (dashed curve) or $\lambda=100$ (solid curve).

As $\tilde{q}$ decreases from $\tilde{q}_2$ to $\tilde{q}_t$, the "acoustical plasmon peak" in the loss function $S(\tilde{q},\tilde{\omega})$ degenerates and ultimately disappears at $\tilde{q}_t$. This degeneration is revealed in Figs. 2(a) and 2(b). In Fig. 2(a) we plot $S(\tilde{q},\tilde{\omega})$ versus $\tilde{\omega}$ for $\lambda=10$ and $\tilde{q}=\tilde{q}_2$; that is, along a line passing through the point ● on curve $A1$ in Fig. 1. We call the smaller peak the "acoustical peak" and the higher peak the "optical peak." Figure 2(b) shows $S(\tilde{q},\tilde{\omega})$ versus $\tilde{\omega}$ for $\lambda=10$ along the line passing through the point ● on the $O1$ curve of Fig. 1, namely $\tilde{q}=0.0175$. The optical peak has shifted to smaller $\tilde{\omega}$ and the acoustical peak has disappeared.

For each of the curves in Fig. 1, we use a + to indicate the point $(\tilde{q}_1,\tilde{\omega}_1)$ at which $\gamma_q/\omega_q=\frac{1}{4}$ and a ● for the point $(\tilde{q}_2,\tilde{\omega}_2)$ at which $\gamma_q/\omega_q=\frac{1}{2}$. The values of $\tilde{q}_1$, $\tilde{\omega}_1$, $\tilde{q}_2$, and $\tilde{\omega}_2$ for the three optical branches, as well as for the three acoustical branches, are given in Table I.

In Fig. 2(c) we compare the plasmon peaks for $\lambda=10$ (dashed curve) to those for $\lambda=100$ (solid curve). In both cases, $\tilde{q}=0.11$, which is $\tilde{q}_2$ for branch $A1$. The $\lambda=100$ optical peak extends to $S(\tilde{q},\tilde{\omega})=40.61$ at $\tilde{\omega}_q=0.309$.

Figures 1 and 2 and Table I display the destruction by scattering of both optical and acoustical plasmons at small q and ω, and show that the wavelength at which these collective modes become overdamped depends strongly on the scattering strength. Figure 1 also shows that the dispersion of those plasmons that are not destroyed by scattering depends only weakly on scattering rates. However, the plasmon lifetime can be considerably reduced by scattering. This is clearly revealed by examining Fig. 2(c), and also by comparing the curves in Fig. 1 and the γ_q/ω_q ratios given in Table II.

In addition to using the loss-function method, we have calculated the dispersion and lifetime for acoustical plasmons in the case $\lambda=10$ in the weak-damping approx-

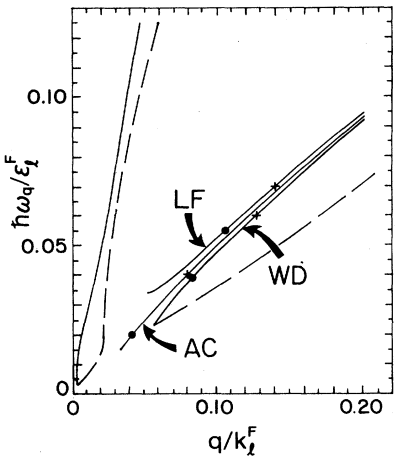

FIG. 3. Comparison of acoustical plasmon dispersions obtained using the loss-function (LF), weak-damping (WD), and analytical continuation (AC) methods. The other solid curve is the optical plasmon dispersion in the weak-damping approximation; the dashed curves indicate other solutions of Eq. (2.4). The symbols + and ● have the same meaning as in Fig. 1.

TABLE I. Points on various optical (Oi) or acoustical (Ai) branches where $\gamma_q/\omega_q=\frac{1}{4}$ [point $(\tilde{q}_1,\tilde{\omega}_1)$] or $\gamma_q/\omega_q=\frac{1}{2}$ [point $(\tilde{q}_2,\tilde{\omega}_2)$]; $i=1$, 2, or 3 signifies $\lambda=10$, 100, or 1000. The branches were determined using the loss-function method, except for $A1$(WD), where the weak-damping approximation was used, and $A1$(AC), where the analytic continuation method was used. Branches $O1$, $O2$, $A1$, and $A2$ are shown in Fig. 1; branches $A1$(WD) and $A1$(AC) appear in Fig. 3.

Branch	$\tilde{q}_1$	$\tilde{\omega}_1$	$\tilde{q}_2$	$\tilde{\omega}_2$
$O1$	6.0×10^{-2}	2.0×10^{-1}	1.8×10^{-2}	8.9×10^{-2}
$O2$	6.0×10^{-4}	1.8×10^{-2}	1.5×10^{-4}	7.7×10^{-3}
$O3$	6.0×10^{-6}	1.8×10^{-3}	1.5×10^{-6}	7.7×10^{-4}
$A1$	1.4×10^{-1}	7.0×10^{-2}	1.1×10^{-1}	5.5×10^{-2}
$A2$	2.3×10^{-2}	1.2×10^{-2}	1.5×10^{-2}	8.4×10^{-3}
$A3$	2.5×10^{-3}	1.4×10^{-3}	1.6×10^{-3}	9.1×10^{-4}
$A1$(WD)	1.3×10^{-1}	6.1×10^{-2}	8.3×10^{-2}	4.0×10^{-2}
$A1$(AC)	8.2×10^{-2}	4.0×10^{-2}	4.3×10^{-2}	2.0×10^{-2}

imation and via the analytic continuation method. The resulting dispersions are indicated in Fig. 3 by the three solid curves situated near the diagonal.[13] The fourth (higher-frequency) solid curve corresponds to the optical branch obtained in the weak-damping approximation, while the two dashed curves indicate other solutions of Eq. (2.4) that are *not* associated with sharp peaks in the loss function.[14,15] The symbols + and ● have the same meaning as in Fig. 1; the associated values of $\tilde{q}$ and $\tilde{\omega}$ are given in Table I.

As expected on general grounds, the three methods yield similar dispersions and lifetimes only when γ_q/ω_q is small. We emphasize that, when employing any of these three methods, meaningful information is obtained only if *both* the dispersion and lifetime are calculated.[16] It is not surprising that the values $\tilde{q}_1$, $\tilde{\omega}_1$, $\tilde{q}_2$, and $\tilde{\omega}_2$ differ considerably for the different methods (Table I).

In the case of strongest scattering considered here ($\lambda=10$), acoustical plasmons are overdamped for $\tilde{q}\lesssim0.10$. Vignale has shown that, for the same values of M, K, and r_h^s used here, short-range exchange-correlation effects limit the existence of acoustical plasmons to $\tilde{q}\leq\tilde{q}_{\max}\approx0.33$, and that the value of $\tilde{q}_{\max}$ can decrease considerably as r_h^s increases.[11] The combination of both disorder-induced electron scattering and exchange-correlation effects may be such as to severely limit, or even destroy, the regime of existence of well-defined acoustical plasmons.

Our results have an important bearing on the question of whether or not acoustical plasmons could mediate the attractive electron-electron interaction in high-T_c superconductors. Mahan and Wu, for example, have concluded that long-wavelength acoustical plasmons are not responsible for the attractive interaction, but have left open the question of the role played by larger-q modes.[10] Our work indicates that, if the scattering is strong enough, then not only very-small-q modes are destroyed, but so are acoustical plasmons of intermediate q. Consequently, a quantitative treatment of such scattering is needed in order to establish the possible role of acoustical plasmons in high-T_c superconductivity.

IV. CONCLUSIONS

Electron-impurity scattering destroys long-wavelength optical and acoustical plasmons in a two-component, quasi-two-dimensional electron gas. The scattering rate strongly affects the critical wave number q_c above which plasmons exist, adjusts the dispersion of surviving plasmons only slightly, and can significantly reduce the plasmon lifetime. Theoretical studies designed to deter-

TABLE II. Comparison of $\tilde{\omega}_q$ and the ratio γ_q/ω_q as a function of $\tilde{q}$ for the acoustical plasmon dispersion curves $A1$ and $A2$ shown in Fig. 1. The lines designated by superscripts * and † denote the smallest values of $\tilde{q}$ for which the peaks associated with $A1$ and $A2$, respectively, have a half maximum on both sides [see Figs. 2(a) and 2(b)]. The lines designated by superscripts ** and ‡ denote the values of $\tilde{q}$ at which the branches $A1$ and $A2$ terminate (see Fig. 1).

	$A1$		$A2$	
$\tilde{q}$	$\tilde{\omega}_q$	γ_q/ω_q	$\tilde{\omega}_q$	γ_q/ω_q
0.2000	0.0947	0.146	0.0939	0.0474
0.1500	0.0736	0.222	0.0725	0.0612
0.1050*	0.0540	0.518	0.0524	0.0812
0.0525**	0.0339		0.0275	0.132
0.0250			0.0136	0.238
0.0200			0.0110	0.306
0.0150†			0.008 36	0.530
0.0075‡			0.004 53	

mine the role played by acoustical plasmons in high-temperature superconductivity must include electron scattering. Finally, experimental detection of acoustical plasmons in quasi-two-dimensional electron systems can be successful only in a range of wave numbers exceeding q_c, but also below the threshold of Landau damping.

ACKNOWLEDGMENTS

One of us (M.R.A.S.) wishes to acknowledge useful discussions with Dr. S.H. Payne. This work was supported financially by the Natural Sciences and Engineering Research Council of Canada.

[1]J. G. Bednorz and K. A. Müller, Z. Phys. B **64**, 189 (1986).

[2]M. K. Wu, J. R. Ashburn, C. J. Torng, P. H. Hor, R. L. Meng, L. Gao, Z. J. Huang, Y. Q. Wang, and C. W. Chu, Phys. Rev. Lett. **58**, 908 (1987).

[3]D. Olego, A. Pinczuk, A. C. Gossard, and W. Wiegmann, Phys. Rev. B **25**, 7867 (1982); R. Sooryakumar, A. Pinczuk, A. C. Gossard, and W. Wiegmann, *ibid.* **31**, 2578 (1985); A. Pinczuk, M. G. Lamont, and A. C. Gossard, Phys. Rev. Lett. **56**, 2092 (1986).

[4]See also G. E. Santoro and G. F. Giuliani, Phys. Rev. B **37**, 937 (1988), and references therein.

[5]J. Ruvalds, Phys. Rev. B **35**, 8869 (1987).

[6]V. Kresin, Phys. Rev. B **35**, 8716 (1987).

[7]Z. Tešanović, Phys. Rev. B **36**, 2364 (1987).

[8]J. Ashkenazi, C. G. Kuper, and R. Tyk, Solid State Commun. **63**, 1145 (1987).

[9]J. I. Gersten, Phys. Rev. B **37**, 1616 (1988).

[10]G. D. Mahan and J.-W. Wu, Phys. Rev. B **39**, 265 (1989).

[11]G. Vignale, Phys. Rev. B **38**, 811 (1988).

[12]G. F. Giuliani and J. J. Quinn, Phys. Rev. B **29**, 2321 (1984).

[13]The curve AC in Fig. 3 does not, in fact, terminate as shown. Severe numerical instabilities are encountered in attempting to solve Eqs. (2.6) and (2.7) beyond the lowest point on the curve. Since there is no physical information to be gained by extending the curve, we forgo the task.

[14]That solutions of Eq. (2.4), such as those shown by dashed curves in Fig. 3, do not correspond to collective excitations, has been emphasized by others as well. See, for example, F. C. Schaefer and R. von Baltz, Z. Phys. B **69**, 251 (1987), and J. Oliva and N. W. Ashcroft, Phys. Rev. B **29**, 1067 (1984). See also J. Appel and A. W. Overhauser, Phys. Rev. B **26**, 507 (1982), and A. W. Overhauser and J. Appel, *ibid.* **29**, 1069 (1984). One way to see that such solutions are not collective modes is to use Eq. (2.5) to show that the corresponding γ_q is negative.

[15]We have examined in detail solutions of Eq. (2.4) obtained both analytically and numerically in some limiting cases (e.g., $M \gg 1$). For $1/\tau_j > 0$, $j=(l,h)$, the solutions found having $\gamma_q > 0$ (solid curves in Fig. 3) met with those having $\gamma_q < 0$ (dashed curves) at points where $q > 0$ and $\omega_q > 0$.

[16]Further to this point, see the papers in Ref. 13 and the discussion in Ref. 11.